

A constitutive model for gas hydrate-bearing soils considering hydrate morphology

Hiromasa Iwai¹* and Takaya Kawasaki¹

¹ Department of Civil and Environmental Engineering, Nagoya Institute of Technology, Nagoya, Japan

* iwai.hiromasa@nitech.ac.jp

Introduction

Recently, not only methane hydrates (MHs) but also carbon dioxide hydrates (CDHs) have been attracting attention from the viewpoint of the enhancing methane gas production and CO₂-storage technology. Many researchers have investigated mechanical properties of both MH and CDH-bearing soils (e.g., Hyodo et al., 2014; Miyazaki et al., 2016), and they have found that there are obvious differences in the stress strain relationship and the dilatancy behaviour between MH and CDH-bearing soils. Some researchers have explained that the difference in MH and CDH may come from different types of hydrate morphology as shown in Fig.1 (i.e., Waite et al., 2009). In the present study, we have proposed a constitutive equation considering the hydrate morphology, and then the proposed model is applied to the past experimental results of both MH and CDH-bearing specimens.

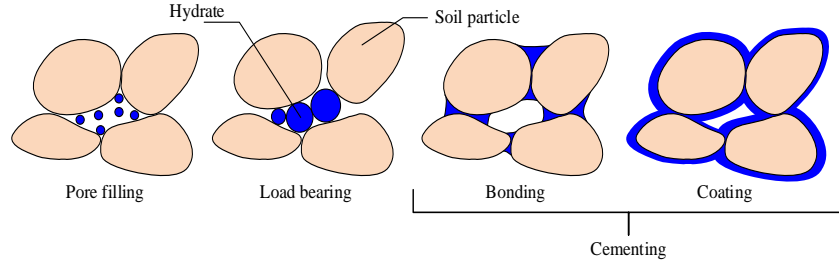


Fig. 1: Schematic view of hydrate morphology and interactions with soil particles

Definition of total hydrate saturation and ratio of each hydrate morphology

In the proposed constitutive model, we assume that there are three different types of hydrate morphology: pore-filling (PF) type, load-bearing (LB) type, and cementing (CM) type, and the total hydrate saturation S_r^H is expressed by the sum of the saturation of each hydrate morphology.

$$S_r^H = S_{CM}^H + S_{LB}^H + S_{PF}^H \quad (1)$$

$$S_{CM}^H = \alpha S_r^H, \quad S_{LB}^H = \beta S_r^H, \quad S_{PF}^H = \gamma S_r^H \quad (\alpha + \beta + \gamma = 1) \quad (2)$$

in which α , β , γ are the ratio of each hydrate morphology with respect to the total hydrate saturation., and the total should be equal to 1.

Yield function and hardening rules

The yield function is given by the following equation. This model is based on the methane hydrate critical state (MHCS) model proposed by Uchida et al. (2012).

$$f = q^2 + M^2 p' [p' - R(p'_c + p'_{CM} + p'_{LB})] \quad (3)$$

where q is the deviator stress, M is the stress ratio at the critical state of host geomaterial, p' is the mean effective stress, and R is the sub-loading surface ratio proposed by Hashiguchi (1989) and its evolution law is given by:

$$dR = -m_R \left\{ (p'_c + p'_{CM} + p'_{LB}) / p'_c \right\} \ln R |d\varepsilon^p| \quad (4)$$

The hardening parameter p'_c is the consolidation yield stress depending on the plastic volumetric strain $d\varepsilon_v^p$, and the conventional evolution law is given by:

$$dp'_c / p'_c = (1 + e) d\varepsilon_v^p / (\lambda - \kappa) \quad (e: \text{void ratio}, \lambda: \text{compression index}, \kappa: \text{swelling index}) \quad (5)$$

In order to express the increase in the strength and dilatancy, we have introduced two different hardening parameters related to GHs, that is, p'_{CM} and p'_{LB} , which are the function of the hydrate saturation of each morphology S_{CM}^H and S_{LB}^H , respectively.

$$p'_{CM} = a_{CM} \left(S_{CM}^H \right)^{b_{CM}}, \quad p'_{LB} = a_{LB} \left(S_{LB}^H \right)^{b_{LB}} \quad (6)$$

in which a_{CM} , b_{CM} , a_{LB} and b_{LB} are the fitting parameters. These parameters are determined so that the material hardening of the CM-type becomes much larger than that of the LB-type: $p'_{CM} > p'_{LB}$.

Material parameters and initial ratio of each hydrate morphology

Table 1 listed material parameters and Table 2 indicates the initial ratio of each hydrate morphology. The initial hydrate morphology ratio is determined so that the proposed model fits the experimental results.

Table 1: Material parameters

p'_0	1.0	ν	0.2	M	1.17	e_0	0.613
λ	0.16	κ	0.004	p'_{c0}	11.0	m_R	15.0
a_{CM}	21.0	b_{CM}	1.0	a_{LB}	6.0	b_{LB}	1.0

Table 2: Initial morphology ratio

	S_r^H	α_0	β_0	γ_0
MH	48.0	0.7	0.2	0.1
CDH	49.0	0.2	0.7	0.1

Model applications and results

The following Fig. 2 indicates a comparison result of the proposed constitutive model with the experimental result presented by Miyazaki et al., (2016); they performed a series of drained triaxial compression tests on both the MH and the CDH-containing sand specimens. The remarkable point in the experiment is that both the strength and the expansive volumetric strain (the volumetric strain is positive in compression) of the MH sand are larger than that of the CDH despite of the total hydrate saturation being almost the same for both. The proposed model well fitted the experimental data by changing the hydrate morphology ratio as indicated in Table 2.

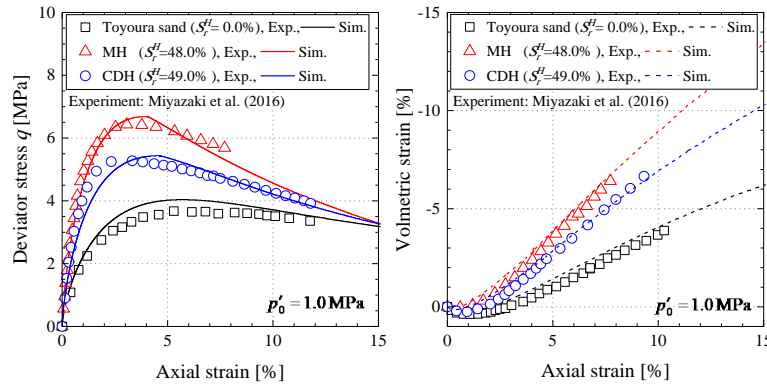


Fig. 2: Comparison of the constitutive model and experimental results of MH and CDH-bearing sand

Conclusion

In the present study, the different types of hydrate morphology were taken into account in the constitutive model for GH-bearing soils, and the model was then applied to the past experiment results. The result indicates that the strength and the dilatancy of MH and CDH-bearing sediments basically depend on the degree of the hydrate saturation. In addition, the hydrate morphology is also one of the key factors which determines the mechanical properties of GH-bearing sediment.

References

- Hashiguchi K (1989) Subloading surface model in unconventional plasticity. *Int. J. Solids Struct.* 25, 917–945
- Hyodo M, Li Y, Yoneda J, Nakata Y, Yoshimoto N, Kajiyama S, Nishimura A, Song Y (2014) A comparative analysis of the mechanical behavior of carbon dioxide and methane hydrate-bearing sediments. *Am. Mineral.* 99, 178–183
- Miyazaki K, Oikawa Y, Haneda H, Yamaguchi T (2016) Triaxial Compressive Property of Artificial CO₂-Hydrate Sand. *Int. J. Offshore Polar Eng.* 26, 315–320
- Uchida S, Soga K, Yamamoto K (2012) Critical state soil constitutive model for methane hydrate soil. *J. Geophys. Res.* 117, B03209
- Waite WF, Santamarina JC, Cortes DD, Dugan B, Espinoza DN, Germaine J, Jang J, Jung JW, Kneafsey TJ, Shin H, Soga K, Winters WJ (2009) Physical properties of hydrate-bearing sediments. *Rev. Geophys.* 47, 1–38